

AN EMI INVERSING PROBLEM FOR LANDMINE CHARACTERIZATION BASED ON IMPROVED PARTICLE SWARM OPTIMIZATION AND FINITE ELEMENT ANALYSIS

Yacine Matriche^{1, 2, 3, *}, Mouloud Feliachi³,
Abdelhalim Zaoui², and Mehdi Abdellah²

¹URD-T, Belfort El-Harrach, Algiers, Algeria

²Ecole Militaire Polytechnique, BP17 B.E.Bahri, Algiers, Algeria

³Université de Nantes, PRES-L'UNAM, IREENA, CRTT, Bd de l'Université, BP 406, 44602 St-Nazaire cedex, France

Abstract—This paper discusses the characterization of landmine by using the electromagnetic induction technique (EMI). The proposed approach is based on the identification of the physical and geometrical properties of a landmine, from the sensor response. But in such an identification, the inverse problem is unavoidable. At first, we begin by simulating the landmine signature by solving a direct problem using the finite element method which constitutes the direct model. After that, we determine the landmine characteristics by using an inverse model based on a cost function optimization. This model is based on an iterative process which coupling finite element analysis and Particles Swarm Optimization (PSO). In this step, we apply two PSO techniques: the Standard PSO (SPSO) and the Improved PSO (IPSO), and discuss the problem of local minima of the cost function. The proposed iterative model is applied to determine the conductivity, geometry, and depth of metallic landmine from its signature measured by EMI. The numerical solution gives good results for the identification of landmine.

1. INTRODUCTION

In recent years, the conflicts in the world have created areas contaminated by landmines or/and Unexploded Ordnance (UXO).

Received 26 December 2012, Accepted 11 March 2013, Scheduled 13 March 2013

* Corresponding author: Yacine Matriche (matriche_yacine@yahoo.fr).

The major problem is that these munitions continue to claim victims even after the conflicts. Some areas in the world are even classified as dangerous and prohibited.

The decontamination of these areas requires the detection by using natural means (dogs, rats, etc...) or technical ones based on GPR or EMI method [1–4].

In the technical methodology, EMI technique is becoming a technology with great potential [4–6]. EMI devices are used either in time domain or frequency one. These systems present a significant difference from the phenomenology of electromagnetic waves because there are no losses in the areas such as water, soil or rocks, which encourages their application in the detection of metallic objects [4].

In the inverse problem, several studies have been undertaken in the frequency domain [7, 8] as well as in the time domain [9, 10]. However, the common point of these researches is the characterization of the buried objects to minimize false alarms due to the presence of non-explosive metallic objects. In this way, several methods have been explored. These developments include the work of [10] in which a separated GPR aperture sensor method is applied to detect buried targets by evaluating and comparing the electromagnetic coupling between the transmitting and receiving antennas. The authors used Finite Difference Time Domain (FDTD) for electromagnetic simulation. In [11], a combined method of the non-uniform fast Fourier transform (NUFFT) migration and the least-square based matching pursuit decomposition (MPD) algorithms were proposed to obtain better discrimination and interpretation for subsurface from ground penetrating radar (GPR) signals. In [12], the researchers applied the normalized surface magnetic charge model overlapping signals to discriminate the objects by using EMI system. In [13], the authors presented a method of buried objects characterization based on a combination of the Method of Auxiliary Sources (MAS) with the Gauss-Newton method of minimization. In [3], the authors introduced the concept of stochastic algorithm for the characterization of UXO. They employed the genetic algorithm combined with GPR system to determine the depth of buried object.

In the present paper, we propose to use an alternate method to solve the EMI inversing problem for the landmine characterization by the combination of the finite element method and IPSO one.

In the first part of this paper, an overview of the studied detection system will be given. In the second part, we will present the Finite Element formulation to get the direct problem solution. Then, the study area will be defined in the third part. The fourth part will be dedicated to the description of the SPSO and IPSO algorithms that will

be used to solve the inverse problem. The local minima problem will also be presented in this section. Afterwards, a comparison between the SPSO and IPSO will be done to validate the influence of the IPSO method on the dodging of particles from local minima. At last, the proposed approach will be validated in the case of various properties (conductivity, depth and radius) of the real buried landmine cases.

2. OVERVIEW OF EMI SYSTEM

2.1. EMI System Description

The basic EMI system consists of a transmitter coil, two receiver coils, power supply, sampling and treatment system [14] (see Figure 1).

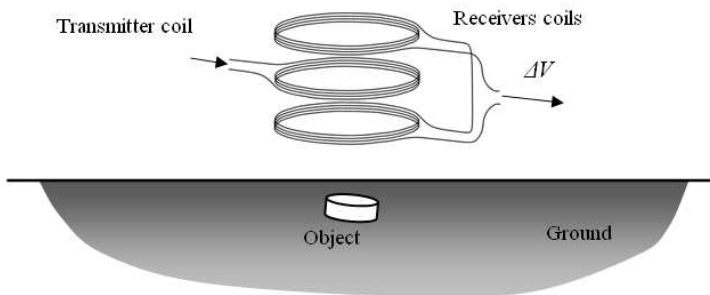


Figure 1. Basic diagram of EMI system.

Its operation is based on electromagnetic induction, where the transmitter coil, traversed by a variable current, will generate an electromotive force across the two receiver coils disposed above and below it. The induced voltage ΔV is zero in the case of no presence of metallic object. During prospecting, when the transmitter coil passes over a metallic object, an eddy current is immediately generated on the surface of the object.

Therefore, these currents will generate an electromotive force which is only across the lower receiver coil. The differential measuring mode eliminates the effect of the exciting field in the two receiving coils, the ΔV depends only on the field generated by the buried object. In this case the ΔV gives the signature of the object since the generated field depends on its physical and geometrical characteristics [15].

The signature of the object must be submissive to a crucial treatment to distinguish the nature of the object and to judge the likelihood of a landmine.

2.2. Domain Geometry and Property

The study area consists of, Figure 2:

- A transmitter coil with a radius of 12 cm is made of 100 windings which carry a current with a density of 2 MA/m^2 .
- Two identical receiver coils with a radius of 10 cm is made of 100 windings. The distance between each of the receiver coils and the transmitter coil is equal of 10 cm.
- The soil is assumed to be homogeneous with an electric conductivity of 0.02 S/m , a relative permittivity of 2.9 and a relative magnetic permeability of 1 [10].
- The landmine is simulated as a vertical cylinder with radius of 5 cm and height of 5 cm, conductivity of 58 MS/m , a relative permittivity of 1 and a relative magnetic permeability of 1. In the first step, the landmine is buried at a depth of 7 cm.
- The EMI system is suspended at a distance of 7 cm from the soil surface.
- The outside area boundaries must be far enough from the field

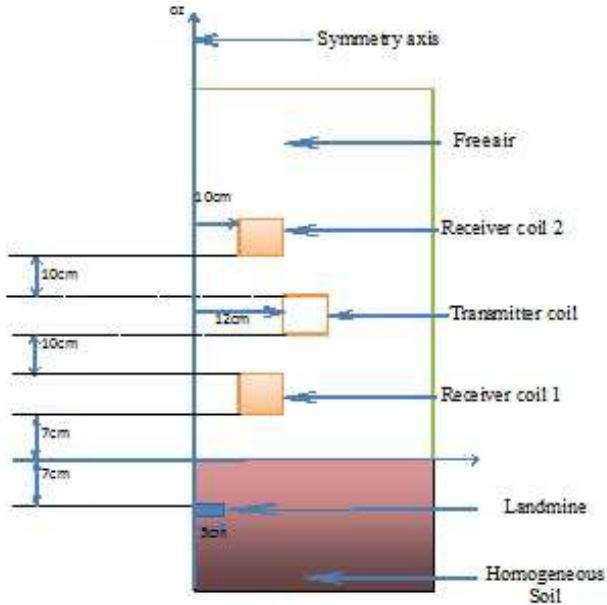


Figure 2. Domain geometry in axisymmetric case.

source to apply homogeneous Dirichlet conditions that will be done in the phase of numerical simulation.

3. SYSTEM MODELING

The EMI modeling is based on Maxwell equation. When using the magnetic vector potential \vec{A} , the direct model is based on the resolution of magnetodynamic equation, given as follow [23]:

$$\vec{\nabla} \wedge \left(\frac{1}{\mu} \vec{\nabla} \wedge \vec{A} \right) + \sigma \frac{\partial \vec{A}}{\partial t} = \vec{J}_s \tag{1}$$

In asymmetrical geometry (Figure 2), we obtain :

$$\frac{1}{\mu} \left(\frac{\partial^2}{\partial r^2} + \frac{\partial^2}{\partial z^2} + \frac{\partial^2}{r \partial r} - \frac{1}{r^2} \right) A_\theta - \sigma \frac{\partial A_\theta}{\partial t} = -J_s \tag{2}$$

where μ , σ , t , (r, θ, z) , and J_s are, respectively, the magnetic permeability, electrical conductivity, time, cylindrical coordinates, and source current density. In asymmetrical coordinates, the vector potential is A_θ . Equation (2) is solved by finite element method to obtain the distribution of magnetic vector potential A_θ in the entire computational domain. The calculation of the voltage V_r , induced in the receiving coils, is given by the following equation:

$$V_r = -\frac{d\phi}{dt} \tag{3}$$

The magnetic flux Φ is given by the curvilinear integral on the length of coil windings:

$$\phi = N_s \int_{\Gamma} \vec{A} d\vec{l} \tag{4}$$

In harmonic case, the induced voltage can be written as:

$$V_r = -j\omega \sum_{i=1}^{N_s} 2 \cdot \pi \cdot r_i A_{\theta,i} \tag{5}$$

where r_i , $A_{\theta,i}$, N_s , and ω represent, respectively, the winding radius of the receiving coil, magnetic vector potential at the center of the windings surface section, number of windings of the receiver coil, and pulsation of the transmitter coil current. In all the following simulations, the current frequency is 1 kHz.

The response of the EMI sensor in differential mode is obtained from the following relation:

$$\Delta V = V_{r1} - V_{r2} \tag{6}$$

where V_{r1} and V_{r2} are, respectively, the induced voltage of the receiver coils above and below the transmitter one.

The identification and localization of buried metallic objects, using the finite element method, requires the consideration of the skin effect on the outer surfaces of the metallic object. To do so, we refine the mesh at those surfaces on a strip of width equal to the skin depth (δ). For a correct representation of the skin effect on the outer surfaces of the object, a mesh, with two layers of triangular elements with a thickness equal to $\delta/2$ for each one, is provided on those surfaces. The skin depth is calculated for each new mesh using the following formula:

$$\delta = \frac{1}{\sqrt{\sigma \cdot \mu \cdot \pi \cdot f}} \quad (7)$$

where: f , σ and μ are, respectively, the current frequency, electrical conductivity, and magnetic permeability of the object.

Note that, if $\delta > d/2$ then δ is fixed to $d/2$, where d is the characteristic dimension of the object.

4. INVERSE PROBLEM

4.1. Domain Geometry and Property

The PSO algorithm is a metaheuristic optimization method of complex systems [16]. It was firstly proposed in 1995 by Kennedy and Eberhart [17] at the international conference on neural networks. It is based on a study of the swarms flight and snow fish group. Initially, these two scientists tried to simulate the ability of birds to fly synchronously and their ability to suddenly change the direction while remaining the optimum formation [18]. The model that the authors of [17] proposed was subsequently extended to a simple and effective optimization algorithm.

During their movement, the particles adjust their new positions by taking into account their velocities at time t , their best performance P_i and the best performance in the whole swarm G_i [17] (see Figure 3).

For each particle, the new velocity V_i and the new position x_i are given as follows:

$$V_i(t+1) = w \cdot V_i(t) + \alpha_1 \cdot r_1 \cdot (P_i - x_i(t)) + \alpha_2 \cdot r_2 \cdot (G_i - x_i(t)) \quad (8)$$

$$x_i(t+1) = x_i(t) + V_i(t+1) \quad (9)$$

where w is a inertia coefficient of the particle, r_1 the cognitive factor that affects the premature convergence to the minimum (global or local), r_2 the social factor that affects exploration of space particles definition, and α_1 and α_2 are random variables taken between 0 and 1.

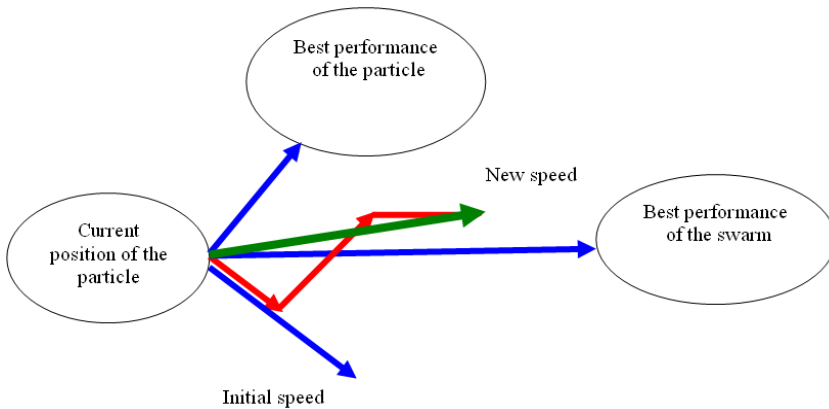


Figure 3. Evaluation of the best particle.

So in the entire iterations, the algorithm will evaluate the cost function for each particle and retain in memory the particle of which the value of the cost function is minimal. This particle will thus be the best particle G_i of the swarm. At the same time, each particle retains its best performance throughout the optimization process P_i .

4.2. Improved Particle Swarm Optimization (IPSO)

The critical problem in PSO optimization is the local minimum of the cost function. During evolution, the particle can be trapped in a local minimum and unable to escape. Indeed, the simple version of the PSO algorithm is not capable of releasing the particle trap in a local minimum. There will be a great influence on the convergence of particles towards the global minimum. To overcome this problem, we make use of three tools to improve the Simple-PSO algorithm.

Firstly, we add a modification to the inertia factor w of the particle to reduce its speed gradually as it approaches the global or local minimum in order to refine the exploration of the space area.

This factor is calculated as follows [19]:

$$w = w_{\max} - \frac{w_{\max} - w_{\min}}{NbIter} \cdot Iter \tag{10}$$

where w_{\max} and w_{\min} are maximum and minimum values of the inertia factor respectively (in our case $w_{\max} = 0.5$ and $w_{\min} = 0.3$). $NbIter$ is the maximum number of iterations and $Iter$ is the current iteration number.

The second improvement is based on the work presented in [20]. Each particle will tend to follow its best performance P_i and the best

performance of the whole swarm G_i . However, all particles tend to follow the same direction. This will have a negative effect on the exploration of the entire space definition. However, by adjusting the two parameters P_i and G_i , each particle will follow a different direction, allowing the swarm to explore the whole domain of definition. The method is based on the discard of the velocity vector, so the new position of the particles is evaluated:

$$x_i(t+1) = w \cdot x_i(t) + \alpha \cdot r_1 \cdot r_3 \cdot (P_i - x_i(t)) + \alpha \cdot r_2 \cdot r_4 \cdot (G_i - x_i(t)) \quad (11)$$

where:

$$r_3 = \begin{cases} 1 & t < T_0 \\ \alpha \cdot (0.8 + 0.2 \cdot r_5) & t \geq T_0 \end{cases} \quad (12)$$

$$r_4 = \begin{cases} 1 & t < T_1 \\ -\alpha \cdot (0.8 + 0.2 \cdot r_6) & t \geq T_1 \end{cases} \quad (13)$$

$$\alpha = \begin{cases} 1 & r_7 < 0.5 \\ 1 & r_7 \geq 0.5 \end{cases} \quad (14)$$

r_3 and r_4 are the disturbed coefficients, and T_0 and T_1 are the disturbed threshold valve values. Let $T_0 = 3$, $T_1 = 3$, r_5 , r_6 and r_7 be random $[0, 1]$. Equation (11) is the External Extremum Disturbed Simple Particle Swarm Optimization (edsPSO) [20]. Thirdly, the black hole model (BHM) is introduced to accelerate the convergence speed PSO algorithm [21]. In the vicinity of the current optimal particle, a small region with radius r and threshold p (p random $[0, 1]$) is generated as a black hole (we take r and p equal, respectively, to 0.00001 and 0.1). Then, a probability l ($l \in [0, 1]$) is randomly generated to every particle of swarm. Provided $l \leq p$, position of the particle is updated by Equation (15).

$$x_i(t+1) = G_i(t) + s \quad s \in [-r, r] \quad (15)$$

Otherwise, the particle escapes from the black hole and is updated by Equation (11).

4.3. Running Algorithm

First, we use the finite element modelling to simulate the measured value of the induced voltage ΔV_{mesu} . Subsequently, we define swarm of particles wherein each particle is a x_i vector whose components are the electrical conductivity, depth and radius of the landmine. This swarm is distributed homogeneously in the space area of definition of the following parameters as:

$$\begin{cases} \sigma \in [0, 100] \text{ MS/m} \\ \text{Depth} \in [1, 40] \text{ cm} \\ \text{Radius} \in [1, 40] \text{ cm} \end{cases} \quad (16)$$

The cost function in this case is the standard deviation between the measured value and the calculated value of ΔV for each particle as follows:

$$F = \sqrt{(\Delta V_{mesu})^2 - (\Delta V_{cal})^2} \quad (17)$$

The proposed method can be summarized in the following organizational chart.

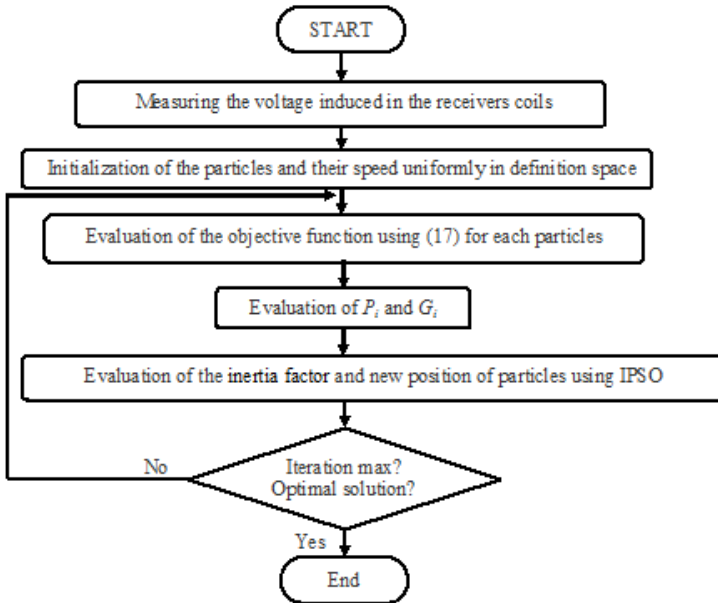


Figure 4. Organizational chart of the method.

It should be noted that during the execution of the program, the skin depth is recalculated for each particle of the swarm based on the electrical conductivity and magnetic permeability values. So the mesh will be adjusted automatically for each particle of the swarm.

5. RESULTS AND DISCUSSIONS

To validate our algorithm (Figure 4), we applied it in order to estimate conductivity, depth and radius of landmine that has the following characteristics:

- Conductivity of 58.6 MS/m.
- Radius of 5 cm.
- Buried at 7 cm under soil.

5.1. Finite Element Simulation

Because of the symmetry of the study domain, the solution is calculated in a reduced domain. We use boundary homogeneous Dirichlet condition to the limit of study area, and also in symmetry axis because the potential vector inside is zero [23]. In the outer surfaces of the metallic object, we refine the mesh to take into account the skin effect (see Figure 5).

Figure 6 shows the equipotential lines created by the transmitter coil without the presence of metallic landmine. These lines have a uniform shape because there is no object that can disrupt these lines. Therefore, induced voltages in receivers coils are the same, thus the difference is null.

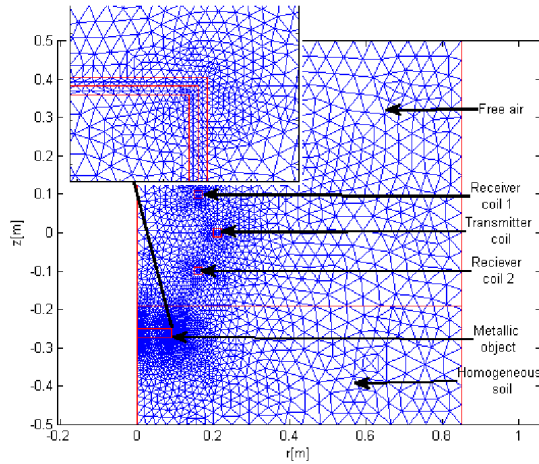


Figure 5. The mesh of the solution domain.

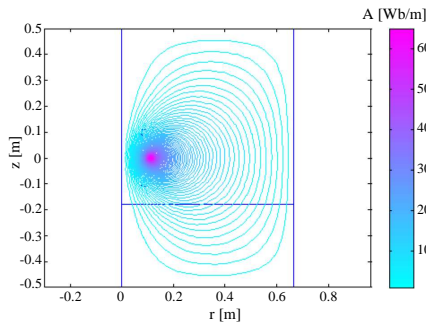


Figure 6. The equipotential lines without the metallic object.

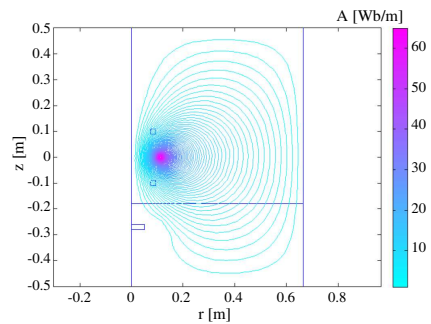


Figure 7. Equipotential lines in the presence of a landmine.

Figure 7 shows the equipotential lines in the presence of a metallic landmine. We note that the metallic landmine influences these lines. Indeed, the current in the transmitter coil will create eddy currents on the surface of the landmine, and the principle of the reaction against the current will in turn create a field that will be opposite to the primary field. This fact reveals the signature of the landmine.

5.2. Inversing Problem Using SPSO

Table 1 shows the parameters used in the inverse problem using the SPSO.

Figure 8 shows the evolution of the particles in definition domain. We note that in the first case the particles converge to the solution who gives the global minimum. This is not the case in most tests. Indeed, for the same test performed several times, in most cases, the particles converge to the nearest local minimum. Figures 9 and 10 show the case in which the particles converge to different local minima.

Table 1. SPSO parameters.

Parameter	Values
<i>Max iteration number NbIter</i>	150
<i>Particles Number</i>	30
<i>Coefficient of inertia w</i>	0.5
<i>Cognitive factor r₁</i>	0.69
<i>Social factor r₂</i>	0.59

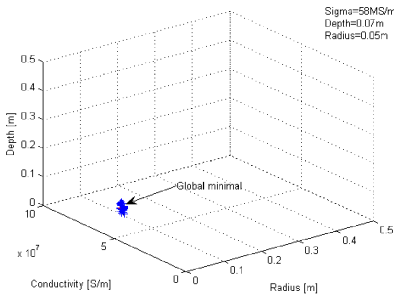


Figure 8. Case where all swarm converges to the global minimum using SPSO.

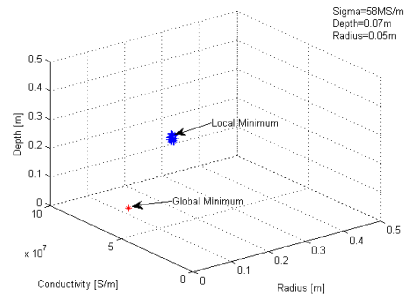


Figure 9. Case where all swarm converges to the local minimum using SPSO (1st case).

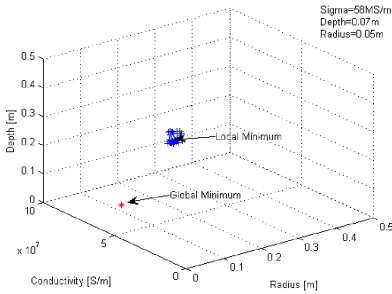


Figure 10. Case where all swarm converges to the local minimum using SPSO (2nd case).

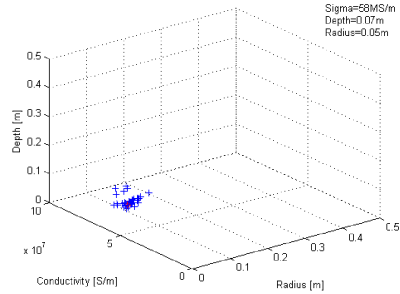


Figure 11. Using IPSO-all swarm converges to the global minimum.

Table 2. IPSO parameters.

Parameter	Values
<i>Max iterations number NbIter</i>	150
<i>Particles Number</i>	30
<i>Max inertia Coefficient w_{\max}</i>	0.5
<i>Min inertia Coefficient w_{\min}</i>	0.3
T_0	3
T_1	3
r	0.00001
p	0.1

5.3. Inversing Problem Using IPSO

To overcome the problem of local minima, we make use the IPSO method. Table 2 shows the parameters used in the inverse problem using IPSO.

Note that in Figure 11, whole swarm converges to the global minimum. We performed the same test 100 times, the result remains the same.

Table 3 shows a comparison between the SPSO and IPSO inversing problem. Note that for the same number of iterations, the IPSO converges 100%. However, the convergence of SPSO is 48%.

Note that the inversion problem using IPSO gives good results.

Table 3. IPSO and SPSO comparison.

Parameters	SPSO	IPSO
<i>Max iteration number NbIter</i>	300	300
<i>Particles Number</i>	30	30
<i>Test number</i>	100	100
<i>Landmine conductivity [MS/m]</i>	58	58
<i>Landmine radius [m]</i>	0.05	0.05
<i>Landmine depth [m]</i>	0.07	0.07
<i>Convergence percentage</i>	48	100

5.4. IPSO Validation Examples

To validate the inversion method, we conducted the test for different objects to identify different parameters.

5.4.1. Case of Real Landmines Simulations

To validate the inversion method, we conducted the same test for different real cases of metallic landmines. The characteristics of each landmine is summarized in Table 4 [22]. Those landmines were considered at different depths. We noticed that the inversion gave good results (see Figure 12).

Table 4. Specification of the landmine [22].

Spec	KM15	KM16
<i>Radius [m]</i>	0.333	0.103
<i>Material</i>	Metal	Metal
<i>Conductivity [MS/m]</i>	10.1	10.1

5.4.2. Case of Different Metallic Object Identification

To generalize the method, we propose in this section to identify the electrical conductivity and the relative magnetic permeability of objects with the following properties:

- Conductivity $\sigma = 58.6$ MS/m; relative magnetic permeability $\mu_r = 100$.
- Conductivity $\sigma = 5.86$ MS/m; relative magnetic permeability $\mu_r = 10$;

- Conductivity $\sigma = 0.586 \text{ MS/m}$; relative magnetic permeability $\mu_r = 1$;

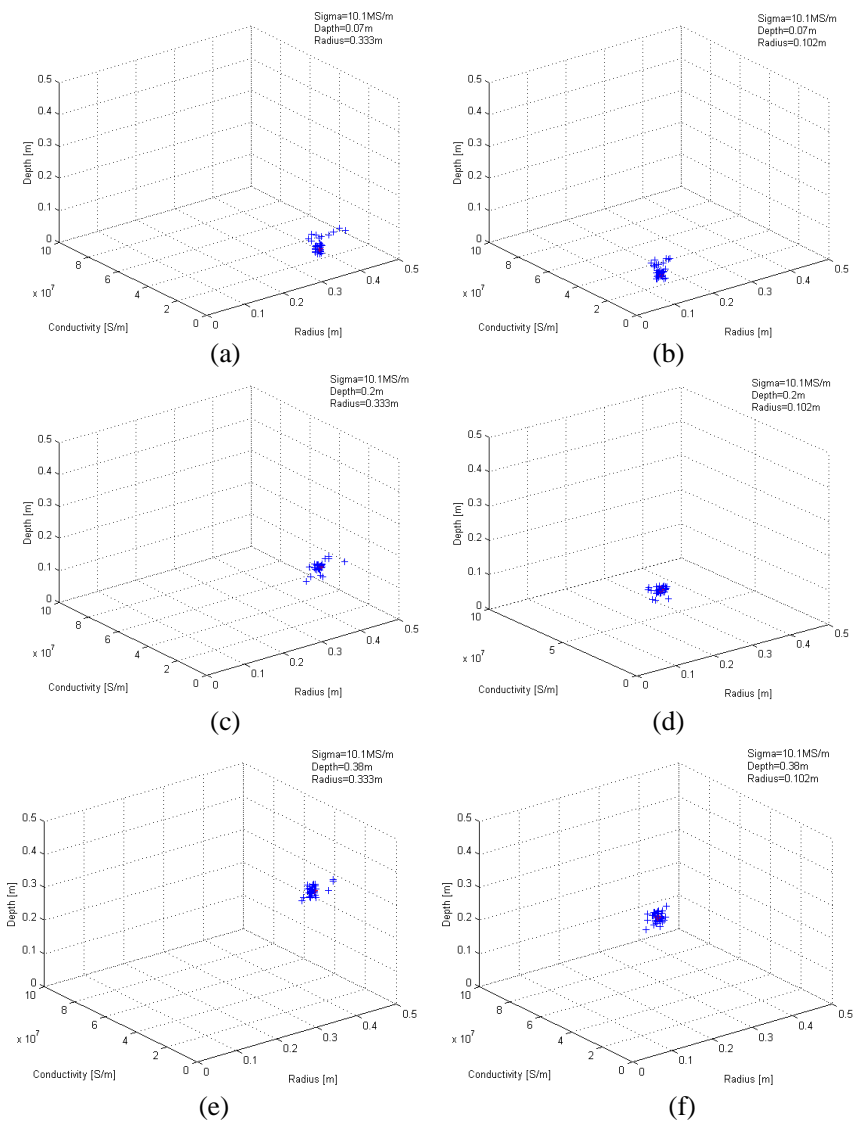


Figure 12. Examples of using IPSO algorithm in the real landmine cases. (a) Landmine KM15 at Depth = 0.07 m. (b) Landmine KM16 at Depth = 0.07 m. (c) Landmine KM15 at Depth = 0.2 m. (d) Landmine KM16 at Depth = 0.2 m. (e) Landmine KM15 at Depth = 0.38 m. (f) Landmine KM16 at Depth = 0.38 m.

Subsequently, we define swarm of particles wherein each particle is a x_i vector whose components are the electrical conductivity and the relative magnetic permeability of the object. This swarm is distributed homogeneously in the space area of definition of the parameters as:

$$\begin{cases} \sigma \in [0, 100] \text{ MS/m} \\ \mu_r \in [1, 120] \end{cases} \quad (18)$$

In this cases, we preserve the other conditions (*radius* = 0.09 m, *height* = 0.025 m and *buried deep* = 0.07 m).

It may be noted that for the first and second cases in Figure 13 and Figure 14, all particles converge to the global minimum. In the third case (Figure 15), the particles do not converge in a precise manner

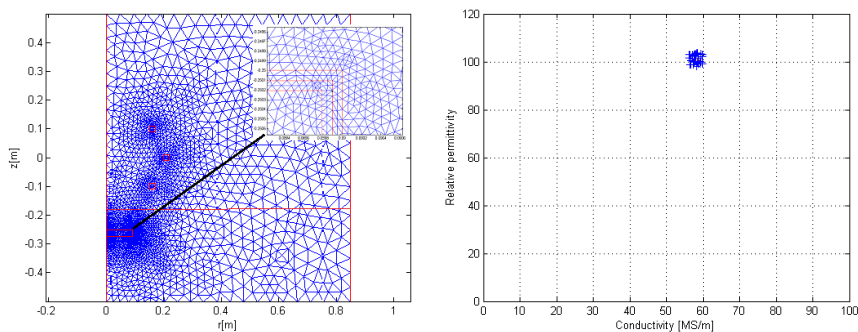


Figure 13. Examples of using IPSO algorithm-object with $\sigma = 58.6 \text{ MS/m}$, $\mu_r = 100$ and $\delta = 2e - 4 \text{ m}$.

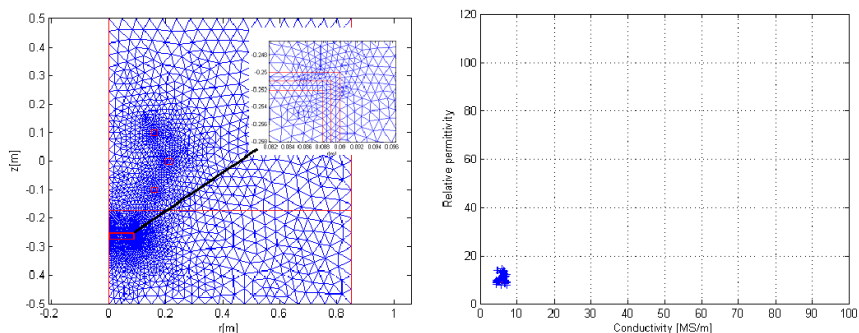


Figure 14. Examples of using IPSO algorithm-object with $\sigma = 5.86 \text{ MS/m}$, $\mu_r = 10$ and $\delta = 0.0021 \text{ m}$.

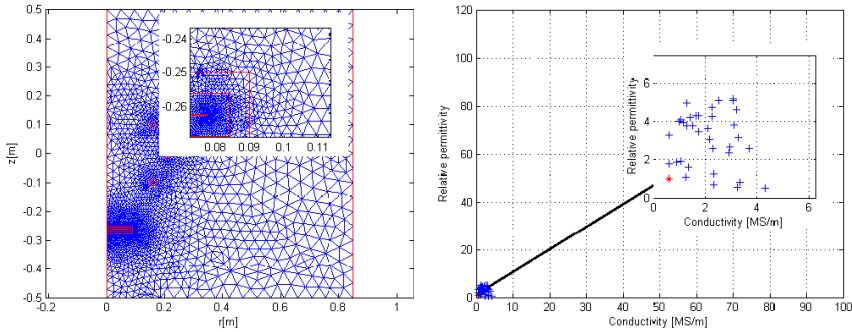


Figure 15. Examples of using IPSO algorithm-object with $\sigma = 0.586$ MS/m, $\mu_r = 1$, and $\delta = 0.0208$ m (then $\delta = 0.0125$ m).

to the global minimum and remain dispersed, because for low values of conductivity, the method is less accurate. In this case, a variation of the conductivity does not involve a significant change in the cost function. Indeed, the EMI system does not allow detection of object with low conductivity.

6. CONCLUSION

In the proposed approach, we have coupled the PSO algorithm to Finite Elements analysis to identify a buried object from its EMI signature. At first, we used the finite element method to collect the signature of the landmine. Secondly, in order to revolve inverse problem, we have associated SPSO algorithm with Finite Element Method. However, we have noticed that SPSO gives aleatory results because of local minima of the cost function. To solve this problem we have introduced IPSO method to help the particles to escape from the trap of local minimum. Several cases of buried object have been tested for the identification of various parameters related to it. The proposed algorithm gives good results. As perspective, we propose to generalize the method for various object geometries.

REFERENCES

1. Wang, Y., Q. Song, T. Jin, Y. Shi, and X.-T. Huang, "Sparse time-frequency representation based feature extraction method for landmine discrimination," *Progress In Electromagnetics Research*, Vol. 133, 459–475, 2013.

2. Throckmorton, C. S., S. L. Tantom, Y. Tan, and L. M. Collins, "Independent component analysis for UXO detection in highly cluttered environments," *Journal of Applied Geophysics*, Vol. 61, No. 3–4, 304–317, Mar. 2007.
3. Tiwari, K. C., D. Singh, and M. K. Arora, "Development of a model for detection and estimation of depth of shallow buried non-metallic landmine at microwave X-band frequency," *Progress In Electromagnetics Research*, Vol. 79, 225–250, 2008.
4. Mahmoudi, M. and S. Y. Tan, "Depth detection of conducting marine mines via eddy-current and current-channeling response," *Progress In Electromagnetics Research*, Vol. 90, 287–307, 2009.
5. Collins, L., C. E. Baum, and L. Carin, "Sensing of unexploded ordnance with magnetometer and induction data: Theory and signal processing," *IEEE Transactions on Geoscience and Remote Sensing*, Vol. 41, No. 5, 1005–1015, May 2003.
6. Pasion, L. R. and D. W. Oldenburg, "A discrimination algorithm for UXO using time domain electromagnetics," *Journal of Environmental and Engineering Geophysics*, Vol. 6, No. 2, 91, 2001.
7. O'Neill, K., F. Shubitidze, I. Shamatava, and K. D. Paulsen, "Accounting for the effects of widespread discrete clutter in subsurface EMI remote sensing of metallic objects," *IEEE Transactions on Geoscience and Remote Sensing*, Vol. 44, No. 1, 32–46, Jan. 2006.
8. Miller, J. T., T. H. Bell, J. Soukup, and D. Keiswetter, "Simple phenomenological models for wideband frequency-domain electromagnetic induction," *IEEE Transactions on Geoscience and Remote Sensing*, Vol. 39, No. 6, 1294–1298, Jun. 2001.
9. Asten, M. W., "On the time-domain electromagnetic response of a conductive permeable sphere," *Journal of Applied Geophysics*, Vol. 67, 63–65, 2009.
10. Moustafa, K. and K. F. A. Hussein, "Aperture sensor GPR system for land mine detection," *Progress In Electromagnetics Research*, Vol. 72, 21–37, 2007.
11. Huang, Y., Y. Liu, Q. H. Liu, and J. Zhang, "Improved 3-D GPR detection by nufft combined with MPD method," *Progress In Electromagnetics Research*, Vol. 103, 185–199, 2010.
12. Shubitidze, F., K. L. O'Neil, B. E. Barrowes, I. Shamatava, J. P. Fernández, K. Sun, and K. D. Paulsen, "Application of the normalized surface magnetic charge model to UXO discrimination in cases with overlapping signals," *Journal of Applied Geophysics*, Vol. 61, 292–303, 2007.

13. Kakulia, D., K. Tavzarashvili, G. Chelidze, and F. Shubitidze, "Inversion of soil's and immersed objects's electromagnetic parameters simultaneously," *DIPED-2009 IEEE Proceedings*, Vol. 978-1, 4244–4201, 2009.
14. Won, I. J., "Characterization of UXO-like targets using broadband electromagnetic induction sensors," *IEEE Transactions on Geoscience and Remote Sensing*, Vol. 41, No. 3, 652–663, Mar. 2003.
15. Huang, H., B. SanFilipo, A. Oren, and I. J. Won, "Coaxial coil towed EMI sensor array for UXO detection and characterization," *Journal of Applied Geophysics*, Vol. 61, No. 3–4, 217–226, Mar. 2007.
16. Wang, W.-T., S.-X. Gong, Y.-J. Zhang, F.-T. Zha, J. Ling, and T. Wan, "Low RCS dipole array synthesis based on algorithm, MOM-PSO hybrid," *Progress In Electromagnetics Research*, Vol. 94, 119–132, 2009.
17. Kennedy, J. and R. C. Eberhart, "Particle swarm optimization," *IEEE International Conference on Neural Networks*, Vol. 4, 1942–1948, Perth, Australia, Jan. 1995.
18. Zhang, Y., S. Wang, and L. Wu, "A novel method for magnetic resonance brain image classification based on adaptive chaotic PSO," *Progress In Electromagnetics Research*, Vol. 109, 325–343, 2010.
19. Li, W.-T., X.-W. Shi, L. Xu, and Y.-Q. Hei, "Improved GA and PSO culled hybrid algorithm for antenna array pattern synthesis," *Progress In Electromagnetics Research*, Vol. 80, 461–476, 2008.
20. Zhang, S., S.-X. Gong, Y. Guan, P.-F. Zhang, and Q. Gong, "A novel IGA-EDSPSO hybrid algorithm for the synthesis of sparse arrays," *Progress In Electromagnetics Research*, Vol. 89, 121–134, 2009.
21. Zhang, J., K. Liu, Y. Tan, and X. He, "Random black hole particle swarm optimization and its application," *IEEE International Conference on Neural Networks and Signal Processing*, 359–365, Jun. 2008.
22. Park, K., S. Park, K. Kim, and K. H. Ko, "Mumti-feature based detection of landmines using ground penetrating radar," *Progress In Electromagnetics Research*, Vol. 134, 455–474, 2013.
23. Pepper, D. and J. C. Heinrich, *The Finite Element Method-basic Concepts and Applications*, Taylor and Francis Group, New York, 2006.